



## OPEN ACCESS

## EDITED BY

Sadik Bay,  
Memorial Sloan Kettering Cancer Center,  
United States

## REVIEWED BY

Hugo Varela-Rodríguez,  
Autonomous University of Chihuahua, Mexico  
Turan Demircan,  
Mugla University, Türkiye  
Nese Aysit,  
Istanbul Medipol University, Türkiye

## \*CORRESPONDENCE

Fernando García-González  
✉ fergarcia202041@cuautitlan.unam.mx

RECEIVED 27 November 2024

ACCEPTED 13 March 2025

PUBLISHED 28 April 2025

## CITATION

García-González F, Servín E,  
Álvarez-Guerrero AL, Alcantar-Rodríguez A  
and Medrano A (2025) Embryo development  
in Mexican axolotl (*Ambystoma mexicanum*):  
a stage morphological study.  
*Front. Amphib. Reptile Sci.* 3:1535817.  
doi: 10.3389/famrs.2025.1535817

## COPYRIGHT

© 2025 García-González, Servín,  
Álvarez-Guerrero, Alcantar-Rodríguez and  
Medrano. This is an open-access article  
distributed under the terms of the [Creative  
Commons Attribution License \(CC BY\)](#). The  
use, distribution or reproduction in other  
forums is permitted, provided the original  
author(s) and the copyright owner(s) are  
credited and that the original publication in  
this journal is cited, in accordance with  
accepted academic practice. No use,  
distribution or reproduction is permitted  
which does not comply with these terms.

# Embryo development in Mexican axolotl (*Ambystoma mexicanum*): a stage morphological study

Fernando García-González<sup>1\*</sup>, Erika Servín<sup>1,2</sup>,  
Alma Lilia Álvarez-Guerrero<sup>3</sup>, Alicia Alcantar-Rodríguez<sup>1</sup>  
and Alfredo Medrano<sup>1</sup>

<sup>1</sup>Faculty of Superior Studies Cuautitlan (UIM – L2), National Autonomous University of Mexico, Cuautitlan Izcalli, Mexico, Mexico, <sup>2</sup>Programa de Doctorado en Ciencias de la Producción y la Salud Animal, National Autonomous University of Mexico (UNAM), Mexico, Mexico, <sup>3</sup>Faculty of Sciences, National Autonomous University of Mexico, Ciudad de México, Mexico

*Ambystoma mexicanum* is an amphibian critically endangered, however is an important model for regeneration research. In this work we analyze axolotl embryo development, identifying and describing the stages from zygote until hatching with high quality images. The embryos were maintained in natural conditions at 16°C, inside their jelly layers the whole study period to take images that show the natural development from oviposition to hatching. We analyzed and described a total of 49 development stages that were grouped in 5 phases: (1) fertilized oocyte, (2) cleavage, (3) gastrulation, (4) neurulation, and (5) organogenesis. Time from fertilization to hatching took about 350 hours under the management conditions set up in laboratory; it can be considered that the complete development of the axolotl embryo until hatching takes two weeks approximately. Results of this work may allow researchers in developmental biology, as well as those working on the conservation of the species including assisted reproduction techniques, to have recent material to carry out studies that favor the understanding and conservation of this Mexican species.

## KEYWORDS

axolotl, embryo development, *Ambystoma mexicanum*, amphibian development, embryo jelly layers

## 1 Introduction

The Mexican axolotl (*Ambystoma mexicanum*) is a urodele amphibian, endemic to the Mexico basin. It is classified as a “Critically Endangered” species in its native habitat by the International Union for Conservation of Nature (IUCN, 2020); this is due to its habitat destruction by pollution and urbanization and also by the introduction of invasive species (SEMARNAT, 2018). This species has been relevant in the Mexican culture and is globally well known as a model to study tissues such as limb regeneration (Bryant et al., 2017).

Even though regeneration and genetic studies have been carried out recently in *A. mexicanum*, there are other biological topics that have no current information such as embryo development. The first reports on this subject were carried out from 1975 to 1989 (Schreckenberg and Jacobson, 1975; Bordzilovskaya et al., 1989).

To make a complete and accurate description of *A. mexicanum* embryo development, we have considered the basic stages of embryonic development described in the literature that focused on amphibians. Once amphibian oocytes are fertilized, the entry of the sperm into the oocyte will determine the dorsal–ventral axis of the embryo; that is, the entry site will become the animal pole representing the ventral region of the new individual, while the opposite side will become the vegetal pole giving rise to the dorsal region of the embryo (Alberts et al., 2014). In the first stages, there is a reorganization of the cellular components in which the microtubules and centrioles of the sperm are involved, which generate a rotation of 30° on the equator of the embryo, developing the gray crescent (Gilbert, 2014). Amphibians present uneven holoblastic segmentation because the vegetal pole contains

a greater quantity of yolk that decreases the segmentation rate. The first cleavage divides the egg into two equal parts, two blastomeres, along a meridional plane that passes through both animal and vegetal poles, beginning with the formation of a groove or fissure at the animal pole (Puente, 1958). The second division occurs in a meridional plane, perpendicular to the first division, resulting in four equal blastomeres. In the third division, the cleavage groove does not occur exactly at the equator but is displaced toward the animal pole, shaping eight blastomeres (Puente, 1958; Gilbert, 2014). In this stage, a faster segmentation is observed in the animal pole, which causes those cells to look smaller in size (micromeres), while in the vegetal pole, cells are larger in size (macromeres) (Richter and King, 2013); thus, the embryo looks asymmetrical (Nieuwkoop and Faber, 1994) (Figure 1). Cell divisions then continue and the blastomeres increase in number, but not in size due to the absence of cell growth between divisions, until they form a morula of 16 to 64 cells, followed by the transition to the blastula stage, when the embryo has 128 cells (Etkin, 1988).

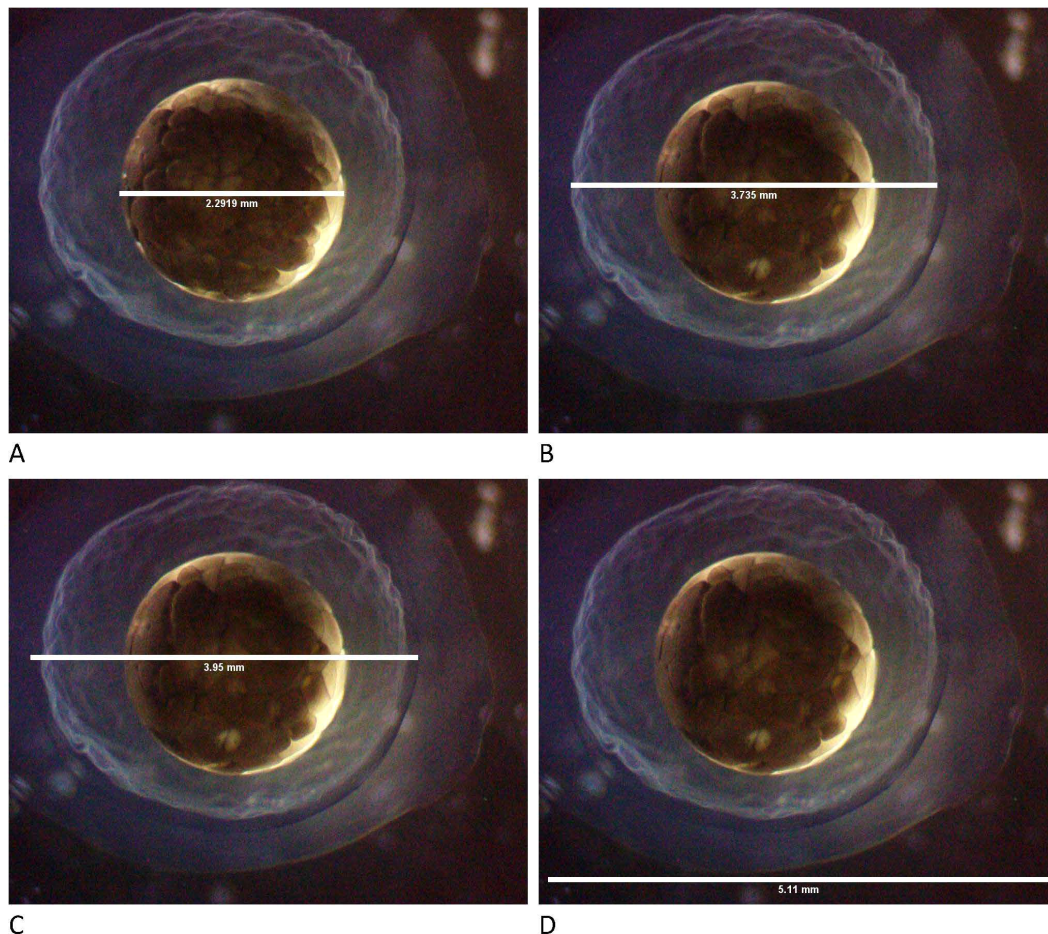


FIGURE 1

Measurements of the embryo and its covering layers of *Ambystoma mexicanum*. (A) Embryo diameter, (B) diameter of the inner layer, (C) diameter of the middle layer, and (D) diameter of the outer layer.

The blastula has an internal cavity known as blastocoel, and at this stage, maternal genes begin to be replaced by genes from the zygote in a process known as mid-blastula transition (Gilbert, 2014). Regulatory factors, such as transcription factors and epigenetic regulators, play a key role in this transition; the arrangement of blastomeres and the formation of the blastocoel are regulated by specific cellular and molecular signals, such as proteins from the Wnt and BMP families (Etkin, 1988). In addition, numerous cell adhesion molecules hold the blastomeres together, with EP-cadherin being one of the most important (Richter and King, 2013).

In gastrulation, the blastula reorganizes through movements of invagination, involution, and epiboly, forming a gastrula with three well-differentiated germinal layers: ectoderm, mesoderm, and endoderm (Keller, 2005), with the dorsal lip of the blastopore being the main gastrulatory center (Gilbert, 2014). During gastrulation, various morphogens act on cell differentiation regulating the dorsal–ventral axis: Wnt/ $\beta$ -catenin and BMP/Noggin pathways, signals that will give rise to different tissues such as Sonic Hedgehog (Shh), Notch, and Hox genes, which have been described in amphibians, mainly in *Xenopus laevis* (Stocum, 1992). The gastrula takes on an elongated and slightly convex shape in the dorsal part of the ectoderm due to the formation of the neural plate extended from the dorsal lip of the blastopore toward the anterior part of the embryo. The transverse and lateral neural folds are formed, forming the neural tube that will give rise to the central nervous system; at this point, it is considered a neurula stage (Puente, 1958). Finally, the ectoderm will give rise to the central nervous system, epidermis, and glandular tissue, among others; the mesoderm will give rise to systems such as the muscular, skeletal, urinary, and blood systems, while the endoderm will give rise to more internal organs such as the digestive and respiratory systems (Roberts, 2000; Gilbert, 2014).

In general, the embryo of *A. mexicanum* measures on average 2 mm and is contained in three well-defined jelly layers. In the early

stages of development, the difference between the animal pole and the vegetal pole is visible (Figure 2) (Bordzilovskaya et al., 1989).

The incubation and complete embryonic development of *A. mexicanum* lasts between 9 and 19 days depending on the ambient temperature (Duhon, 1992; Nugas and Byrant, 1996). To carry out a successful incubation, it is necessary to maintain water quality with the physicochemical parameters recommended for this species, including NO<sub>2</sub> (0–40 mg/L), NO<sub>3</sub> (0–1 mg/L), NH<sub>3</sub> + NH<sub>4</sub> (0–0.5 mg/L), and pH (7–8.4) (Mena and Servín, 2014). Additionally, the use of solutions with balanced mineral concentrations for the incubation of embryos has been described, specifically in *A. mexicanum* (Nugas and Byrant, 1996), using the modified Holtfreter's solution (NaCl 0.059 M, KCl 0.0067 M, CaCl<sub>2</sub> 0.00076 M, and NaHCO<sub>3</sub> 0.0024 M), showing success in the incubation of embryos in laboratory conditions.

In this work, we studied the embryonic development of the Mexican axolotl (*A. mexicanum*) as part of our line of research focused on the conservation of the species through gamete and embryo cryopreservation. This information may be useful for different assisted reproduction techniques. For this, we monitored the embryo development of the Mexican axolotl throughout incubation, and then employing high-quality photographs, we examined and analyzed the main and distinctive morphological characteristics of the embryos. The objectives of this work were to expand and update the information reported by previous authors and that findings from this study provide useful information for future research work in cryopreservation processes.

## 2 Methods

This work was conducted at the Multidisciplinary Research Unit (Reproduction Laboratory and Vivarium) of the Faculty of Superior Studies Cuautitlan (FESC), National Autonomous University of Mexico (UNAM), Mexico.

### 2.1 Animals and housing

To carry out this project, five males and seven females of Mexican axolotl (*A. mexicanum*) were selected. They were housed at the vivarium, in a 3 × 4-m area specially conditioned for their care; temperature and light/darkness periods were controlled, and their diet was based on pellets and live food. The diet of the breeders was based on the provision of 5 g of live food (*Tubifex tubifex*) twice a week and pelletized food for turtles once a week. Axolotls were housed individually in plastic tubs (15 L capacity) with refuge areas. Cleaning was carried out every third day, using tap water filtered by a five-step reverse osmosis filter (Rotoplas<sup>TM</sup>), maintaining water quality with appropriate conditions for this species: pH 7.8, ammonium 0 ppm, nitrites 0 ppm, and nitrates 5 ppm (Mena and Servín, 2014).

The breeders were selected considering the following characteristics: older than two and a half years, weighing more than 70 g, 25 to 30 cm in total length, and in good health. Natural reproduction was encouraged to obtain the embryos used in this

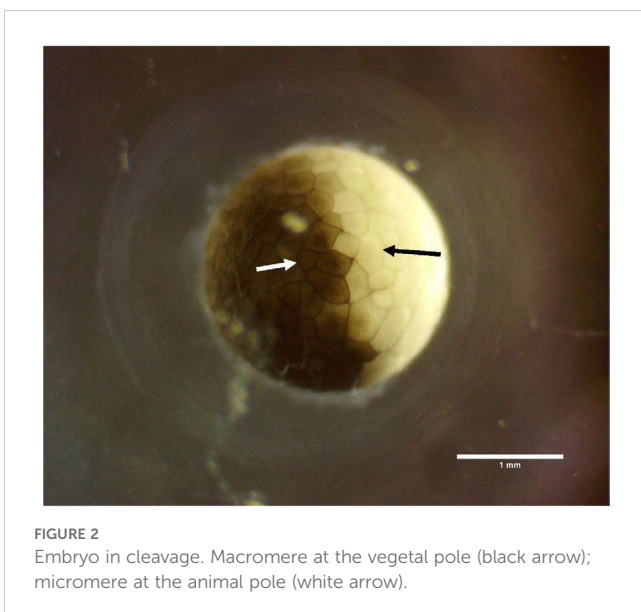


**FIGURE 2**  
Embryo in cleavage. Macromere at the vegetal pole (black arrow); micromere at the animal pole (white arrow).

work. For this, a 200-L aquarium was installed, with a waterfall filter and a chiller (Baoshishan™) with a capacity of 260 L, which allows the temperature to be lowered to 12°C–14°C, thus favoring natural reproductive behavior (Vázquez-Silva, 2020). The behavior of the couple was monitored to verify that courtship would occur. Monitoring and videorecording of reproductive behavior was carried out (EPCOM, SYSPM01V3, Mexico), observing from courtship to oviposition.

Once the female had oviposited, some embryos were carefully removed from the aquarium transporting them to the laboratory in a small container, filled with water from the same tank. Embryos were observed under a stereoscopic microscope to evaluate their morphological characteristics and to select those presenting appropriate characteristics of development.

## 2.2 Embryo assessment

For the selection of embryos used during the study, approximately 20 recently oviposited zygotes were put one by one in a petri dish added with water from the axolotl reproduction tank, where the oviposition took place, and were examined with a stereoscopic microscope (Kyowa, Japan) at ×20 magnification to select those showing normal morphological characteristics: i) presence of the three intact jelly layers with a clear and transparent appearance, discarding those that were opaque or damaged; and ii) spherical embryos with a homogeneous pigmentation. The selected embryos were kept in water at 16°C throughout the evaluation and microphotography.

Embryo development was monitored from the moment it was laid until the exact moment of larval hatching. The photographic record was made with a software (Amscope version x64, 3.7) connected to a digital camera for microscopy (USB Digital Camera OPT-14mp), and a time lapse was programmed in the software to take photographs every 10 min; images were ordered by following the classification of axolotl embryo development stages reported by Schreckenberg and Jacobson (1975).

## 3 Results

In this work, we identified a total of 49 stages of axolotl embryo development that were grouped into five phases: 1) fertilized oocyte, 2) cleavage, 3) gastrulation, 4) neurulation, and 5) organogenesis. The time from fertilization to hatching took approximately 350 h (range: 312–388 h) under the management conditions set up in this work.

### 3.1 Stages of embryo development

Next, embryo development was described, focusing on the observable morphological characteristics, and in some cases, additional information, based on bibliography, on what changes occurred internally was provided.

#### 3.1.1 Phase 1: fertilized oocyte—zygote

In this phase, one stage is included:

Stage 1. Zygote is spheric in shape, its surface is homogeneously pigmented, and the place the spermatozoon has penetrated the oocyte is clearly observable: a pigmented point enclosed by a clearer area (Figure 3A1, blue arrow).

#### 3.1.2 Phase 2: cleavage

In this phase, 11 stages are included (2–12):

Stage 2. This stage represents a two-blastomere-segmented embryo in which a segmentation groove, going from the dorsal to the ventral pole, is evident (Figure 3A2, white arrow); blastomeres are symmetric in size.

Stage 3. Second segmentation takes place producing four well-defined symmetric blastomeres (Figure 3A3, white arrow).

Stage 4. Third segmentation takes place, in the equatorial axis, producing four cells in each pole; in this way, the animal pole (ventral) and the vegetal pole (dorsal) are clearly distinguishable (Figure 3A4, red arrow).

Stage 5. The embryo is formed by 16 cells, and this stage until stage 10 is considered a morula; cleavage occurs asynchronously, and cells have a polyhedral appearance. At this point, the segmentation rate of the animal pole is faster than that of the vegetal pole; thus, cells in the animal pole are smaller in size (micromeres) than those in the vegetal pole (macromeres) (Figure 3A5) (Chung and Malacinski, 1983).

Stage 6. The embryo is formed by 32 cells; the difference in size between micromeres and macromeres is more apparent (Figure 3A6, black and green). A cavity starts to form in the interior of the embryo (Puente, 1958).

Stage 7. The embryo is formed by 64 cells; as cleavage progresses, cells are smaller in size, but individual cells are clearly delimited (Figure 3B, white and red arrows).

Stage 8. Each cellular division produces new cells half the size of the previous one but well delimited from one another; it is difficult to count the number of cells (Figure 3B8).

Stage 9. The small size and high number of cells make it difficult counting them; the difference in size between micromeres and macromeres is much more apparent than before (Figure 3B9, green and black).

Stage 10. Cell size continues to decrease, and segmentation grooves between cells clearly delimit from one another (Figure 3B10).

Stage 11. Blastula. Cell size continues to decrease (Figure 3B11) (Hara and Boterenbrood, 1977); the time from stage 10 to 11 takes approximately 15 h, much longer than previously reported (Figure 4).

Stage 12. The number of cells increases, while their size continues to decrease; individual cells are clearly observable (Figure 3B11).

#### 3.1.3 Phase 3: gastrulation

In this phase, six stages are included (13–18):

Stage 13. Gastrula formation. The boundaries between cells, at the animal pole, are not observable; the epiboly process begins (Gilbert, 2014) (Figure 3C13). On the other pole, cells accommodate themselves.

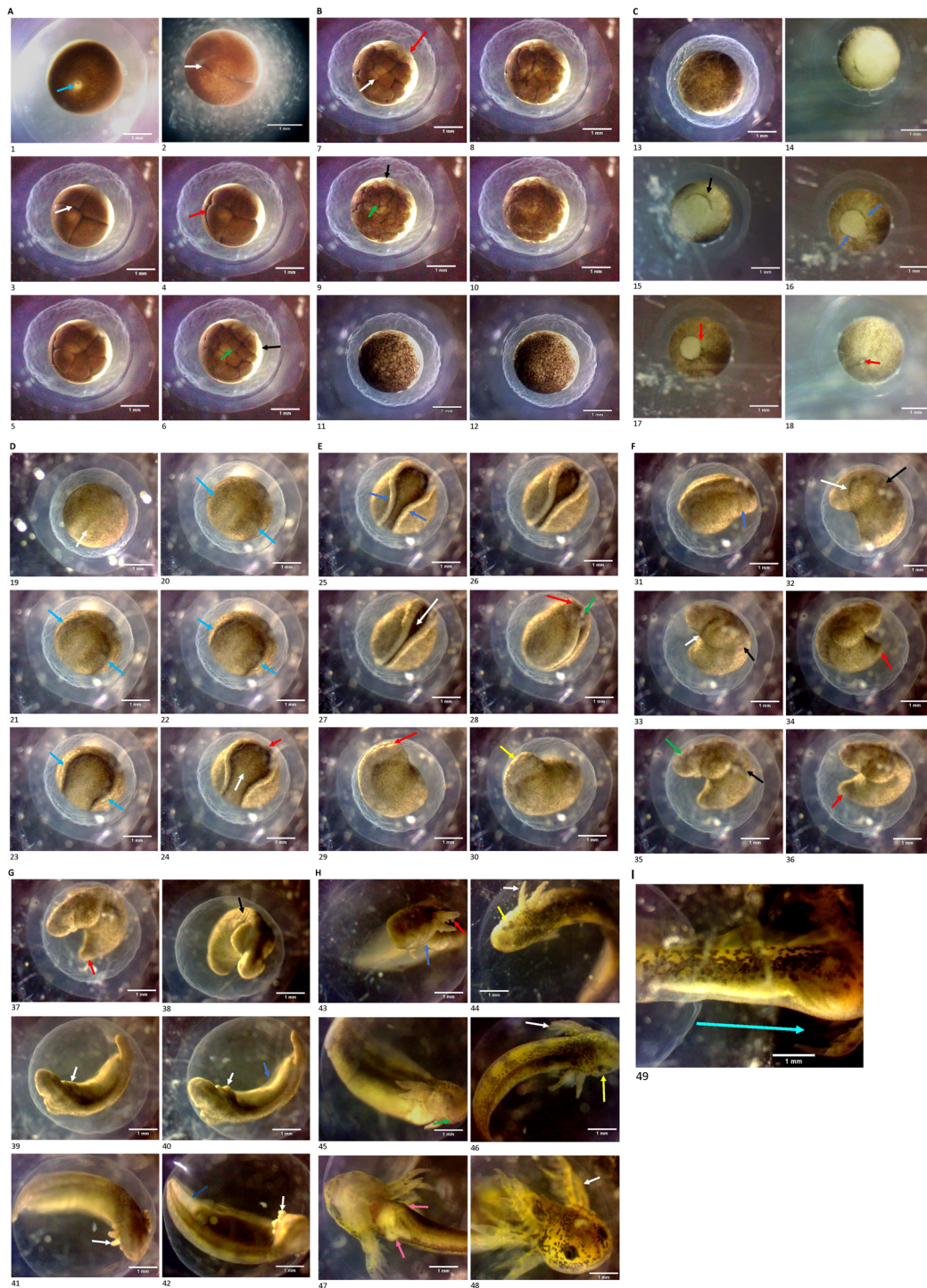


FIGURE 3

(A) Fertilization and cleavage (description in the text). Sperm entry site (blue arrow), cleavage furrow (white arrow), segmentation on the equatorial axis (red arrow), micromere (green arrow), and macromere (black arrow). (B) Cleavage (description in the text). Animal pole (white arrow), vegetal pole (red arrow), micromere (green arrow), and macromere (black arrow). (C) Gastrula (description in the text): early gastrula 13 to 16, middle gastrula 17, and late gastrula stage 18. Dorsal lip of the blastopore (black arrow), lateral lips of the blastopore (blue arrows), and yolk plug (red arrow). (D) Early and intermediate neurulation (description in the text). Neural groove (white arrow), neural folds (blue arrow), and neural crest (red arrow). (E) Intermediate and late neurulation (description in the text). Neural folds (blue arrow); neural tube (white arrow); neural crest (red arrow); rostral neuropore (green arrow); prosencephalon, mesencephalon, and rhombencephalon (yellow arrow). (F) Late neurulation and organogenesis (description in the text). Mandibular groove (white arrow), somites (black arrow), pharyngeal arches (blue arrow), tail bud (red arrow), and head (green arrow). (G) Organogenesis (description in the text). Tail (red arrow), somites (black arrow), gills (white arrow), and dorsal caudal fin (blue arrow). (H) Organogenesis (description in the text). Gills (white arrow), branchial branching (red arrow), eye (yellow arrow), heart (blue arrow), mouth (green arrow), and forelimb (pink arrows). (I) Hatching (description in the text).

Stage 14. Early gastrula. Animal pole cells invaginate to form the dorsal lip, and the vegetal pole becomes pigmented (Figure 3C14) (Barlow, 2001). Stages 14–18 are viewed from the vegetal pole.

Stage 15. The dorsal lip of the blastopore is evident (Figure 3C15, black arrow). Involution and epibolia movements make the external cells move to the embryo interior displacing the blastocoel and favoring the formation of germ layers (endoderm, mesoderm, ectoderm) (Gresens, 2004).

Stage 16. Cellular movements continue, and lateral lips of the blastopore begin to form (Figure 3C16, blue arrows). Inside, the blastocoel is further displaced, and the archenteron from which the primitive digestive tube originated begins to form (Brun and Garson, 1984).

Stage 17. Middle gastrula. The yolk plug is formed (Figure 3C17, red arrow); the ventral lip of the blastopore forms and attaches to the lateral lips, and they all form the yolk plug. Invagination, involution, and epibolia complete the formation of the ectoderm and both the mesoderm and endoderm in the interior (Brun and Garson, 1984).

Stage 18. Late gastrula. The yolk plug becomes smaller in size (Figure 3C18) until its appearance is like a scar; the prechordal plate, which will give rise to the notochord, is formed (Brun and Garson, 1984).

### 3.1.4 Phase 4: neurula

In this phase, 23 stages are included (19–41):

Stage 19. Early neurulae. A groove goes from the anterior to the posterior region, and the neural groove begins to form (Figure 3D19, white arrow); the embryo is pigmented. Specification of the neural plate, neural crest, and epidermis begins; inside the embryo is the notochord that will direct the neurulation process (David and Jacobson, 1990).

Stage 20. Folding of the neural plate begins, and this forms the neural folds at both sides of the embryo, from rostral to caudal direction (Figure 3D20, blue arrows).

Stage 21. Folding of the neural plate continues, producing two dorsal crests or folds (Figure 3D21, blue arrows). Inside the embryo, the notochord pushes cells of the neural plate to produce those structures (Taniguchi et al., 2017).

Stage 22. Neural folds suffer an evident elevation forming the borders of the neural folds (Figure 3D22, blue arrows); this process is more notorious at the rostral than at the caudal region and includes both sides of the embryo.

Stage 23. Neural folds approach each other at the middle part of the embryo (Figure 3D23, blue arrows); this is considered the transition zone between primary (rostral) and secondary (caudal) neurulation.

Stage 24. Neural folds continue approaching each other, and a small line between neural folds along the embryo, from rostral to caudal direction, can be distinguished (Figure 3D24, white arrow); this produces the neural groove. Inside the neural groove, the notochord will be located (Brun and Garson, 1984).

Stage 25. Middle neurula. Dorsal folds continue elevating and converge to form the neural tube (Figure 3E25, blue arrows); not yet closed.

Stage 26. The transition zone of neurulation becomes narrower (Figure 3E26). The inside of the neural plaque is progressively covered by dorsal folds (Taniguchi et al., 2017).

Stage 27. Neural folds have nearly attached to each other, neural crests are more evident, and the neural tube begins to form (Figure 3E27, white arrow).

Stage 28. At the rostral part of the embryo, neural crests are very close to each other (Figure 3E28, red arrow); the rostral neuropore is visible (Figure 3E28, green arrow). From this stage, the embryo starts moving (rotates in its axis); the embryo begins moving to a lateral position, and the neural folds have attached to each other.

Stage 29. Late neurula. Neural folds have fused with each other from the rostral to the caudal part (Figure 3E29, red arrow); the embryo begins to curve. Inside the embryo, once the neural tube is completely closed, the cells of the neural crest disaggregate in the rostral–caudal direction differentiating to other cellular types (Barlow, 2001).

Stage 30. Two ectodermal thickenings, at the embryo cephalic area, can be observed (Figure 3E30, yellow arrow). The prosencephalon, mesencephalon, and (Falk et al., 2002).

Stage 31. Pharyngeal arcs begin to form at the rhombencephalon region (Figure 3F31, blue arrow).

Stage 32. The submandibular groove is apparent (Figure 3F32, white arrow); somites, approximately three pairs, can be observed (Figure 3F32, black arrow).

Stage 33. The submandibular groove becomes more apparent separating the head from the body (Figure 3F33, white arrow); somites are more prominent, and approximately seven pairs can be distinguished (Figure 3F33, black arrow).

Stage 34. The embryo head is more prominent, and the tail is apparent (Figure 3F34, red arrow); rotational movement stops.

Stages 35 to 37. The embryo head becomes progressively more prominent, and the tail gradually elongates (Figure 3F35, 36, G37, green and red arrows).

Stage 38. The embryo continues elongating (Figure 3G38); from this stage until hatching, circular movement of the embryo is evident.

Stage 39. The embryo ventral region decreases in volume, and gill buds are evident as small protuberances (Figure 3G39, white arrow).

Stage 40. The embryo tail becomes thinner and longer in size, and gill buds increase in size (Figure 3G40, white arrow); the dorso-caudal fin begins to develop (Figure 3G40, blue arrow).

Stage 41. Embryo gills are more apparent, and three pairs can be distinguished (Figure 3G41, white arrow).

### 3.1.5 Phase 5: organogenesis

In this phase, eight stages are included (42–49):

Stage 42. Gills are more prominent, and they look folded (Figure 3G42, white arrow).

The dorso-caudal fin is evident and extends from the head to the cloaca (Figure 3G42, blue arrow) (Adamson et al., 2022).

Stage 43. Gills begin to branch out (Figure 3H43, red arrow); heartbeat is clearly observable (Figure 3H43, blue arrow); the embryo becomes progressively pigmented.

Stage 44. Gills are much longer in size, pointed and branched (Figure 3H44, white arrow). The embryo looks like an axolotl, and because it is much larger, it must flex within the jelly layers. The eye region is more evident and pigmented (Figure 3H44, yellow arrow), and the whole embryo shows pigmentation points.

Stage 45. A mouth hint is observable (Figure 3H45, green arrow); gill development continues.

Stage 46. Gills continue branching and elongating (Figure 3H46, white arrow); the eyes are well delimited and protrude from the face surface (Figure 3H46, yellow arrow); the whole body of the embryo is pigmented.

Stage 47. The forelimb buds are visible (Figure 3H47, pink arrows) and will continue developing some days after hatching.

Stage 48. Gills are fully developed and may be expanded as a hand fan (Figure 3H48, white arrow); the mouth and eyes are well defined. The embryo is ready for hatching.

Stage 49. Hatching in progress (Figure 3I49; blue arrow shows the direction the embryo comes out).

Hatched larva and jelly layers keeping their shape are shown in Figures 5A, B.

## 4 Discussion

According to this study, which describes from the fertilization of the oocytes to the hatching of the larvae, we proposed a total of

49 stages, more than those reported by Schreckenberg and Jacobson (1975). Unlike these authors, we have included additional stages (5–12) because our images allowed us to distinguish blastomere segmentation showing a progressive clear reduction in each cell size. In contrast, in the mentioned work, it was not possible to differentiate the limits between individual blastomeres.

Others reported 31 stages according to external anatomical characteristics (Rivera, 2019); in contrast, Holly et al. (2003) reported some stages after hatching, reaching a total of 57, which included the development of the forelimbs and hindlimbs.

It is worth mentioning that this work was based on one individual embryo from three different embryo laying. Embryos were kept all the time in natural conditions within their jelly layers, keeping a constant temperature of 16°C. In contrast, Schreckenberg and Jacobson (1975) removed the embryos from the jelly layers to take photographs; thus, their images showed embryos without any barrier that limited the extension of their body. In our case, embryos within the jelly layers did not have enough space to expand, so they look flexed, which caused the images to be blurred in certain regions. In this work, we decided to reduce the handling of the embryos as much as possible to avoid introducing any artificial change; thus, images showed some blurred areas. In our future work, we will try to improve lighting and optical settings. On the other hand, Holly et al. (2003) fixed embryos in formalin that may cause morphological changes.

The duration of embryogenesis in our work, approximately 350 h at 16°C, was similar to that reported before: from 330 h until the larvae hatched at 18°C (Holly et al., 2003) to 488 h until stage 40, at a constant temperature of 18°C (Schreckenberg and Jacobson, 1975).

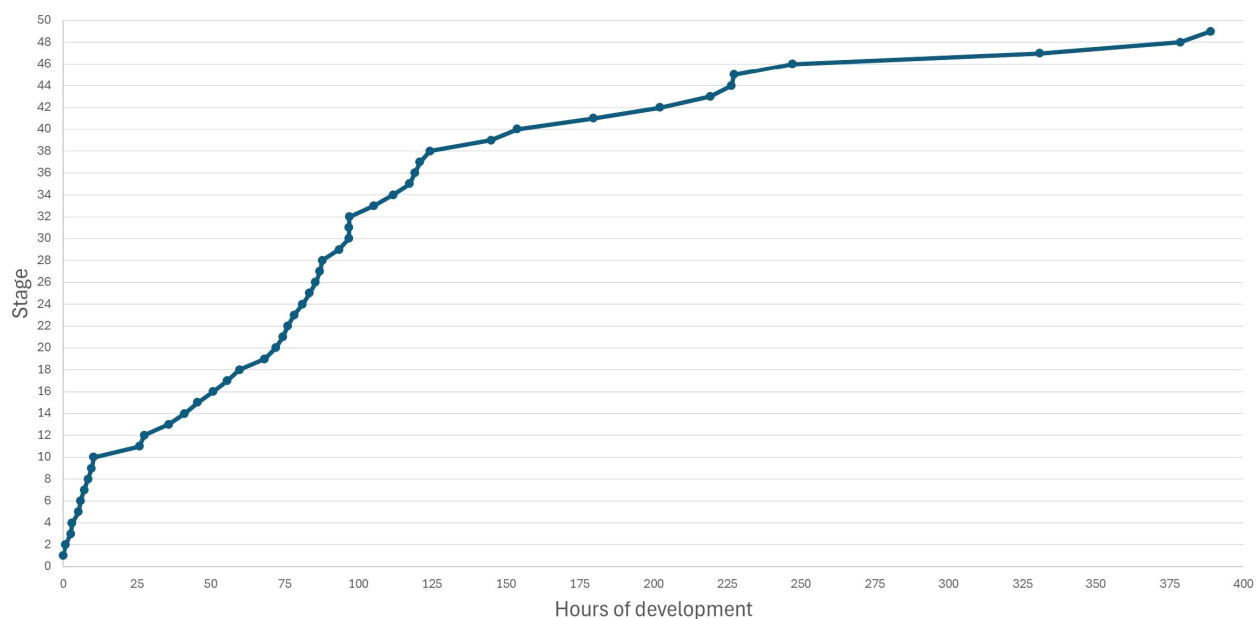


FIGURE 4  
Time of embryo development of *Ambystoma mexicanum*.



A



B

FIGURE 5  
Hatching. (A) Newly hatched larva; (B) jelly layers after hatching.

## 5 Conclusions

The temperature of embryo housing affects embryonic development, and even under the same conditions, each embryo presents a small but different rhythm of development. Despite this difference, it can be considered that the complete development rhythm of the axolotl embryo until hatching takes approximately 2 weeks. It is important to perform more studies for monitoring both external and internal changes of the embryo throughout their development; this may help in understanding and eventually overcome or minimize the

effects that cryopreservation protocols produce in the embryos of *A. mexicanum*.

It is of great interest, that in the future, this study is complemented by histological or molecular techniques, such as PCR and *in-situ* hybridization, among many others that provide us with more detailed information on the genetic and molecular factors involved in embryo development and differentiation and even in the regeneration of the different tissues of the axolotl; with this, we may understand and correlate the external changes observed with the internal changes that we do not review in this work.

## Data availability statement

The raw data supporting the conclusions of this article will be made available by the authors, without undue reservation.

## Ethics statement

The animal study was approved by the Internal Committee for the Care and Use of Experimental Animals (CICUAE-FESC C23-21) of the Faculty of Superior Studies Cuautitlan, National Autonomous University of Mexico. The study was conducted in accordance with the local legislation and institutional requirements.

## Author contributions

FG-G: Conceptualization, Data curation, Investigation, Methodology, Visualization, Writing – original draft, Writing – review & editing. ES: Conceptualization, Data curation, Formal analysis, Methodology, Visualization, Writing – original draft, Writing – review & editing. AA-G: Conceptualization, Data curation, Formal analysis, Investigation, Methodology, Visualization, Writing – review & editing. AA-R: Conceptualization, Data curation, Funding acquisition, Investigation, Supervision, Visualization, Writing – review & editing. AM: Conceptualization, Data curation, Formal analysis, Funding acquisition, Investigation, Project administration, Supervision, Validation, Visualization, Writing – original draft, Writing – review & editing.

## Funding

The author(s) declare that financial support was received for the research and/or publication of this article. This work was supported by Universidad Nacional Autonoma de Mexico (UNAM): PAPIIT

## References

- Adamson, C. J., Morrison-Welch, N., and Rogers, C. D. (2022). The amazing and anomalous axolotls as scientific models. *Dev. Dynam.* 251, 922–933. doi: 10.1002/dvdy.470
- Alberts, B., Johnson, A., Lewis, J., Raff, M., Roberts, K., and Walter, P. (2014). *Molecular Biology of the Cell. 6th edition* (Canada: Garland Science).
- Barlow, L. A. (2001). Specification of pharyngeal endoderm is dependent on early signals from axial mesoderm. *Development* 128, 4573–4583. doi: 10.1242/dev.128.22.4573
- Bordzilovskaya, N. P., Dettlaff, T. A., Duhon, S. T., and Malacinski, G. M. (1989). “Developmental-stage series of axolotl embryos,” in *Developmental Biology of the Axolotl*. Eds. J. B. Armstrong and G. M. Malacinski (Oxford University Press, New York), 201–219.
- Brun, R. B., and Garson, J. A. (1984). Notochord formation in the Mexican salamander (*Ambystoma mexicanum*) is different from notochord formation in *Xenopus laevis*. *J. Exp. Zool.* 229, 235–240. doi: 10.1002/jez.1402290208
- Bryant, D. M., Johnson, K., DiTommaso, T., Tickle, T., Couger, M. B., Payzin-Dogru, D., et al. (2017). A Tissue-Mapped Axolotl De Novo Transcriptome Enables Identification of Limb Regeneration Factors. *Cell Reports* 18, 762–776.
- Chung, H. M., and Malacinski, G. M. (1983). Reversal of developmental competence in inverted amphibian eggs. *J. Embryol. Exp. Morph.* 73, 207–220. doi: 10.1242/dev.73.1.207
- David, J., and Jacobson, A. G. (1990). The origins of neural crest cells in the axolotl. *Dev. Biol.* 141, 243–253. doi: 10.1016/0012-1606(90)90380-2
- Duhon, S. T. (1992). Spawning Axolotls at UI: A ten-year history, *Axolotl newsletter. Summer* 21, 29–36.
- Etkin, L. D. (1988). “Regulation of the mid-blastula transition in amphibians,” in *The Molecular Biology of Cell Determination and Cell Differentiation* (New York: Springer).
- Gilbert, S. F. (2014). *Developmental Biology. 10th Edition* (Sunderland (MA: Sinauer Associates).
- Gresens, J. (2004). An introduction to the Mexican Axolotl (*Ambystoma mexicanum*). *Lab. Anim.* 33, 41–47. doi: 10.1038/labanim1004-41
- Hara, K., and Boterenbrood, E. C. (1977). Refinement of Harrison’s normal table for the morula and blastula of the axolotl. *Wilhelm Roux’ Archiv* 181, 89–93. doi: 10.1007/BF00857270
- Holly, L. D. N., Cameron, J. A., Chernoff, E. A., and Stocum, D. L. (2003). Extending the table of stages of normal development of the axolotl: Limb development. *Dev. Dynam.* 226, 555–560. doi: 10.1002/dvdy.10237
- IUCN (2020). The iucn red list of threatened species. doi: 10.2305/IUCN.UK.2020

IN206524, FESC CI2441. E. Servin received a scholarship (CVU 859019) from the Mexican Government (CONAHCYT).

## Acknowledgments

The authors extend their thanks to the members of the FES Cuautitlán, Multidisciplinary Research Unit Animal Reproduction Lab—Norhan Cortes, Alberto Cardenas, Daniel Gonzalez, Monserrat Torres, Karmina Lopez, Koreim Mendez, Marycruz Martinez, Andres Perez, Alan Martinez, Ulises Garcia, Luz Sanchez, Alejandro Aguirre, Fernanda Ortiz, and Antonio Olvera—for their assistance.

## Conflict of interest

The authors declare that the research was conducted in the absence of any commercial or financial relationships that could be construed as a potential conflict of interest.

## Generative AI statement

The author(s) declare that no Generative AI was used in the creation of this manuscript.

## Publisher’s note

All claims expressed in this article are solely those of the authors and do not necessarily represent those of their affiliated organizations, or those of the publisher, the editors and the reviewers. Any product that may be evaluated in this article, or claim that may be made by its manufacturer, is not guaranteed or endorsed by the publisher.

- Keller, R. (2005). Cell migration during gastrulation. *Curr. Opin. Cell Biol.* 17, 533–541. Available at: [https://www.sciencedirect.com/science/article/pii/S0955067405001092?casa\\_token=UGa3ieMPPEQAAAAA:bH3XhF\\_BH\\_IQOdRmDwPZ75iIDjs4Myl2OS4eDWKmAax7wUU3\\_vWjaBdckJ6rHLuWfUGCyGM\\_dt4p](https://www.sciencedirect.com/science/article/pii/S0955067405001092?casa_token=UGa3ieMPPEQAAAAA:bH3XhF_BH_IQOdRmDwPZ75iIDjs4Myl2OS4eDWKmAax7wUU3_vWjaBdckJ6rHLuWfUGCyGM_dt4p) (Accessed November 20, 2024).
- Mena, H., and Servin, E. (2014). Manual básico para el cuidado en cautiverio del axolote de Xochimilco (*Ambystoma mexicanum*), Manual básico para el cuidado en cautiverio del axolote de Xochimilco (*Ambystoma mexicanum*). doi: 10.22201/ib.9786070255137p.2014
- Nieuwkoop, and Faber, (1994). *Normal Table of Xenopus Laevis (Daudin): A Systematical & Chronological Survey of the Development from the Fertilized Egg till the End of Metamorphosis*. Available online at: <http://Www.Xenbase.Org/Anatomy/Alldev.Do> (Accessed November 25, 2024).
- Nugas, C., and Byrant, S. (1996). Axolotl larvae housing methods. *Axolotl. Newslett.* 25.
- Falck, P., Hanken, J., and Olsson, L. (2002). Cranial neural crest emergence and migration in the Mexican axolotl (*Ambystoma mexicanum*). *Zoology* 105, 195–202.
- Puente, F. (1958). Huevos y Larvas de Anfibios. *Munibe Cienc. Naturales* 10, 325–344.
- Richter, H. K., and King, M. W. (2013). *Amphibian embryology: A laboratory manual* (University of California Press).
- Rivera, I. C. (2019). Seguimiento del desarrollo embrionario y osteogénesis en *Ambystoma mexicanum*.
- Roberts, D. J. (2000). Molecular mechanisms of development of the gastrointestinal tract. *Dev. Dynam.* 219, 109–120. doi: 10.1002/1097-0177(2000)9999:9999<::AID-DVDY1047>3.3.CO;2-Y
- Schreckenberg, G. M., and Jacobson, A. G. (1975). Normal stages of development of the axolotl, *ambystoma mexicanum*. *Dev. Biol.* 42, 391–400. doi: 10.1016/0012-1606(75)90343-7
- SEMARNAT (2018). *Programa de Acción para la Conservación de las Especies Ambystoma spp.* SEMARNAT/CONANP (México). Available online at: [https://www.gob.mx/cms/uploads/attachment/file/444128/PACE\\_Ambystoma2.pdf](https://www.gob.mx/cms/uploads/attachment/file/444128/PACE_Ambystoma2.pdf) (Accessed Jun 18, 2024).
- Stocum, D. (1992). “Dynamics of the Gastrulation Movements and Determination of the Mesoderm in Amphibian Embryos,” in *Morphogenesis: An Analysis of the Development of Form and Pattern in Biological Systems* (New York: Cambridge University Press).
- Taniguchi, Y., Kurth, T., Weiche, S., Reichelt, S., Tazaki, A., Perike, S., et al. (2017). The posterior neural plate in axolotl gives rise to neural tube or turns anteriorly to form somites of the tail and posterior trunk. *Dev. Biol.* 422, 155–170. doi: 10.1016/j.ydbio.2016.12.023
- Vázquez-Silva, G., Arana-Magallón, F. C., López-de la Rosa, A. K., Mendoza-Martínez, G., Martínez-García, J. A., and Hernández-García, P. A. (2020). Evaluación de la reproducción de *ambystoma mexicanum* y *ambystoma velasci* mediante dos formas de aplicación hormonal. *Revista Mexicana De Agroecosistemas* 8, 28–35.